



**ICA 2013 Montreal  
Montreal, Canada  
2 - 7 June 2013**

**Signal Processing in Acoustics**

**Session 1pSPb: Acoustic Feature Extraction and Characterization**

**1pSPb6. Analysis of backward waves and quasi-resonance of shells with the invariants of the time reversal operator.**

**Franck D. Philippe, Dominique Clorennec, Maximin Ces, Romain Anankine and Claire Prada\***

**\*Corresponding author's address: ESPCI ParisTech, CNRS UMR 7587, Institut Langevin - Ondes et Images, 1 rue Jussieu, PARIS, 75005, France, France, [claire.prada-julia@espci.fr](mailto:claire.prada-julia@espci.fr)**

Backward waves propagating on shell are guided modes with opposite phase and group velocities. For a shell in vacuum, backward modes are linked to zero group velocity modes and resonances which have been the object of recent studies. For a shell embedded in water, the group velocity does not vanish because of the leakage into the fluid. However, the group velocity of the backward mode has a minimum associated to a quasi-resonance. These phenomena are studied on air filled steel and zircaloy hollow cylinders, using a 3MHz linear array in pulse echo mode. The circumferential guided modes are generated and their radiation into water detected by the array. The modes are separated using the decomposition of the time reversal operator (TRO), each pair of counter-propagating modes being associated to 2 invariants of the TRO [Prada & al. J. Acoust. Soc. Am. 1998]. Two resonances are revealed by the eigenvalues of the TRO, one is associated with the first longitudinal thickness resonance and the other, very high, occurring at a slightly lower frequency, corresponds to the minimum of the group velocity of the backward mode. The back-propagations of the eigenvectors of the TRO provide the phase velocities of these modes.

Published by the Acoustical Society of America through the American Institute of Physics

## INTRODUCTION

Acoustic scattering by elastic shells have been the object of numerous studies. For thin shells, an enhanced backscattering was observed around the minimum frequency of the  $S_1$  Lamb mode. Sammelman<sup>1</sup> et al. attributed this phenomenon to the quasi-resonance occurring at this minimum. It was then explained by Kaduchak et al.<sup>2,3</sup> by the contribution of the backward mode  $S_{2b}$  having opposite phase and group velocities. This backward mode was observed experimentally by Meitzler<sup>4</sup> and later by Germano & al.<sup>5</sup>. For a shell in vacuum, backward modes exist on a branch joining a thickness mode ( $k=0$ ) (either shear or longitudinal, depending on Poisson's ratio) to a zero group velocity modes ( $k \neq 0$ ). For a shell embedded in water, the group velocity does not vanish due to the leakage into the fluid. However, it has a minimum associated to the quasi-resonance.

To understand these phenomena and their contribution to the enhanced back-scattering, it is interesting to achieve a spatio-temporal analysis of the back-scattered field. Several years ago, we proposed to use the Decomposition of the Time Reversal Operator method (DORT) to analyze the elastic waves radiated by a thin hollow cylinder embedded in water<sup>7</sup>. The method was used to separate the different modes circumnavigating the shell. It was shown that each pair of counter-propagating modes is associated to a pair of invariants of the Time Reversal Operator. In the following, we use the same approach to study higher frequency  $\times$  thickness range where the backward wave  $S_{2b}$  exists. We observe this backward wave as well as the quasi-resonances occurring at the minimum of the group velocity. Measurements were performed on different air filled hollow cylinders revealing similar behaviors. First, the dispersion curves of the backward modes and the radiation of guided modes traveling around a shell are discussed. Then the experimental results obtained with the DORT method on a Zircaloy tube are presented.

## RADIATION OF CIRCUMFERENTIAL GUIDED MODES

When a plane wave incident on an air filled shell is reflected into a specular echo and is converted into guided modes circumnavigating the shell. The modes are generated if the Snell's law is satisfied: the angle of incidence  $\theta$  satisfies the equation  $\sin(\theta) = C_0/C_\phi$  where  $C_0$  is the acoustic velocity in the fluid and  $C_\phi$  the phase velocity of the mode. Then, the mode propagates and radiates into the fluid with the opposite angle. Most modes having a positive phase velocity, turn around the shell before radiating back parallel to the incident direction (Fig.1 left). The mode generated at point A propagates clockwise and radiates back from point B. Because of the symmetry, there is also a mode generated in B which radiates back from A. As shown in Kaduchak<sup>3</sup>, for a backward mode with opposite phase and group velocities, the phenomenon is different. The mode generated in A propagates counter-clockwise a short distance before it radiates in the direction opposite to the incident direction (Fig.1 right). As a consequence, a backward mode loses much less energy before radiating in the direction opposite to the incident one.

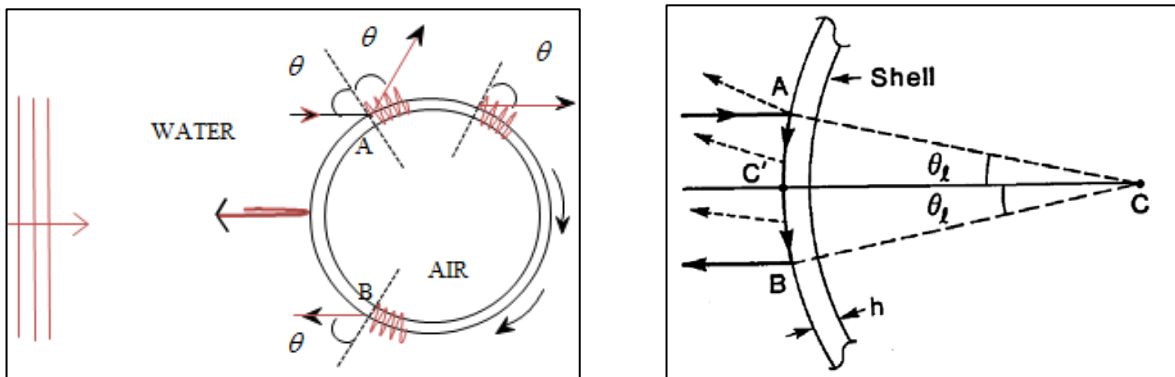


**FIGURE 1.** On the left, generation and radiation of a forward Lamb mode. On the right, generation and radiation of the backward wave  $S_{2b}$  (from Kaduchak<sup>2</sup>). Phase velocity and group velocity being of opposite sign, the generated wave radiates back to the source before circumnavigating the shell.

When an array is used to observe this phenomenon, aperture effects occur. Using a ray approach, it appears that the radiation of the mode towards the array follows rays that are tangential to the circle of radius  $R \sin(\theta)$  ( $R$  is the

cylinder radius). Thus, for a limited array aperture, the radiated field comes from two symmetrical secondary sources separated by the distance  $d=2R.\sin(\theta)$ . The phase velocity of the mode is then provided by the simple formula  $C_\phi = 2RC_0/d$ .

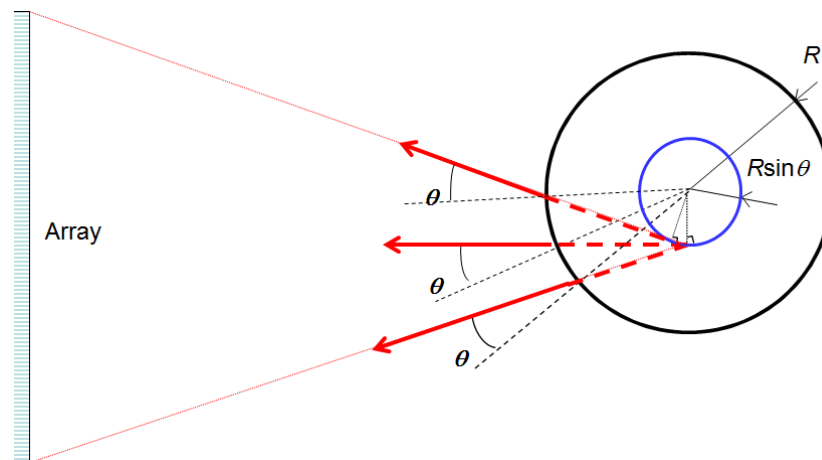


**FIGURE 2.** Radiation of a guided mode of phase velocity  $C_\phi$  into a fluid of velocity  $C_0$  circumnavigating a shell of radius  $R$  (in black). Far enough, the wave appears to radiate from two symmetrical points located on a circle of diameter  $2RC_0/C_\phi$  (in blue).

### Invariants of the Time Reversal Operator

When the backscattering experiment is done in a symmetrical geometry, pairs of counter propagating modes are generated. As shown in Prada and Fink<sup>7</sup>, each pair of counter propagating modes is associated to a pair of invariants of the Time Reversal Operator and corresponds to a pair of secondary sources that are symmetrical with respect to the array axis. The eigenvectors are the responses from these sources oscillating either in phase or out of phase. In reference 7, the experiment was performed on a 0.5 mm thick steel shell of diameter 20 mm with a 128 linear array of 3.5 MHz central frequency. Three Lamb modes were observed, corresponding to  $A_0$ ,  $S_0$  and  $A_1$ . The phase velocities of the modes were determined and the cut off frequency of the  $A_1$  mode estimated. Several turns around the shell of  $S_0$  and  $A_1$  modes were detected, resulting in resonance peaks in the eigenvalue of the time reversal operator.

To determine these invariants, the array response matrix  $k(i,j,t)$  is acquired ( $i,j$  being the element numbers and  $t$  the time). A time window is applied to eliminate the specular echo. The frequency response matrix  $K(i,j,\omega)$  is then obtained by Fourier transform. The singular value decomposition is performed at each frequency. Finally, the singular vectors corresponding to the dominant singular values are back propagated numerically to determine the positions of the associated secondary sources and find the phase velocity of the mode. In most cases, the 2 singular values associated to a pair of modes are close. To obtain a better precision on the secondary sources positions, the sum of the two squared back-propagated fields is used.

### BACKWARD WAVES AND RESONANCES

Backward waves are observed in all isotropic elastic plates. The first backward mode is labeled  $S_{2b}$  because it is linked through a purely imaginary branch to the  $S_2$  mode. For a plate in vacuum, the  $S_{2b}$  mode exists just below the smallest frequency of  $V_T/2d$  and  $V_T/d$  and the minimum frequency of the  $S_1$  mode where the group velocity vanishes (Meitzler<sup>4</sup>). Thus, this mode corresponds to a thickness resonance at its highest frequency (either shear or stretch depending on Poisson's ratio) and to a ZGV resonance at its lowest frequency. Other backward waves exist for higher order Lamb modes but generally on a smaller frequency domain. Often, only the real wave number solutions of the Rayleigh-Lamb equation are represented. In fact, a complex solution starts at the minimum of the  $S_1$  mode corresponding to an evanescent mode (Fig.3, black line).

When the plate is embedded in water, the evanescent mode split into two complex modes as shown on Fig.3. The longitudinal thickness mode with a zero group velocity mode does not exist because of leakage. However, the  $S_{2b}$  mode still exists and starts from the shear thickness resonance at its highest frequency.

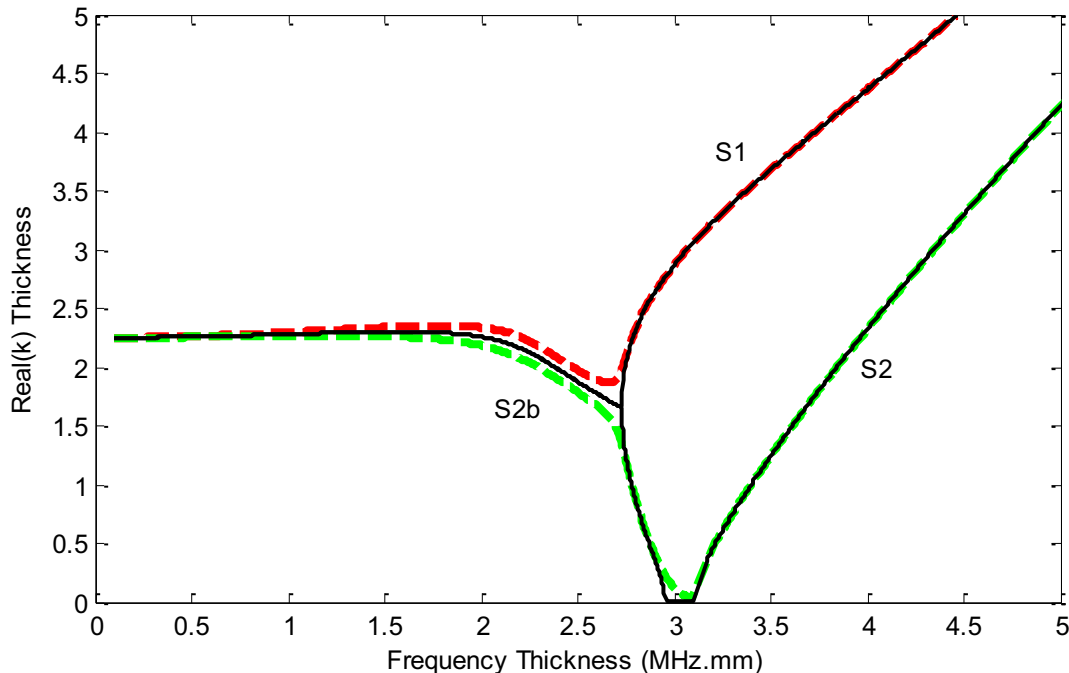


**FIGURE 3.** Dispersion curves of the symmetrical modes for a steel plate : Real part of the complex wave number as a function of frequency. In black, the curves calculated for a steel plate in air, and in green and red the curves calculated for the steel plate in water.

## EXPERIMENTAL RESULTS

Acoustic backscattering from a zirconium tube (external radius 4.75 mm and thickness 0.57 mm) was studied. Zirconium alloy tubes are extensively used for cladding fuel rods in nuclear pressurized water reactors. Thus it is important to control their integrity and they have been the object of several studies in the ultrasonic domain. In a recent paper<sup>8</sup> we have measured by laser ultrasonic means in the air the local resonance spectrum of the zirconium tube associated with different ZGV modes. The elastic properties of the zirconium were then determined assuming transverse isotropy in the plane perpendicular to the cylinder axis. The longitudinal and transverse bulk velocities were measured equal to 4.740 mm/ $\mu$ s and 2.405 mm/ $\mu$ s. For these velocities, the second shear thickness resonance is close to the first longitudinal resonance, so that there is a strong repulsion between the modes  $S_1$  and  $S_2$ . Thus, the ZGV point is at a frequency far below the longitudinal thickness resonance. In the present paper, only circumferential guided modes will be observed, thus the tube will be considered as isotropic. In Ces et al.<sup>8</sup>, it was also shown that the  $S_1$  and  $S_{2b}$  modes were not affected by the curvature of the tube. Using the above velocities, we have calculated the dispersion curves of a plate with air on one side and water on the other side (Figure 4). Because of the leakage, the group velocity of  $S_{2b}$  does not vanish but it has a minimum at a frequency close to the ZGV point. The  $S_{2b}$  mode is linked to the shear thickness resonance at 4.22 MHz, and the longitudinal resonance at 4.15 MHz does not belong to the modes.

Acoustic scattering from the zirconium tube was measured with a 128 transducer array of central frequency 3.5 MHz and pitch 0.417 mm. The array is connected to a 128 channels programmable device (Lecoeur Electronique). The center of the zirconium tube is placed at 62.5 mm from the array. To increase signal to noise ratio, the array response matrix is acquired using the Hadamard Walsh basis. The circumferential guided modes are generated and their radiation into water detected by the same array.

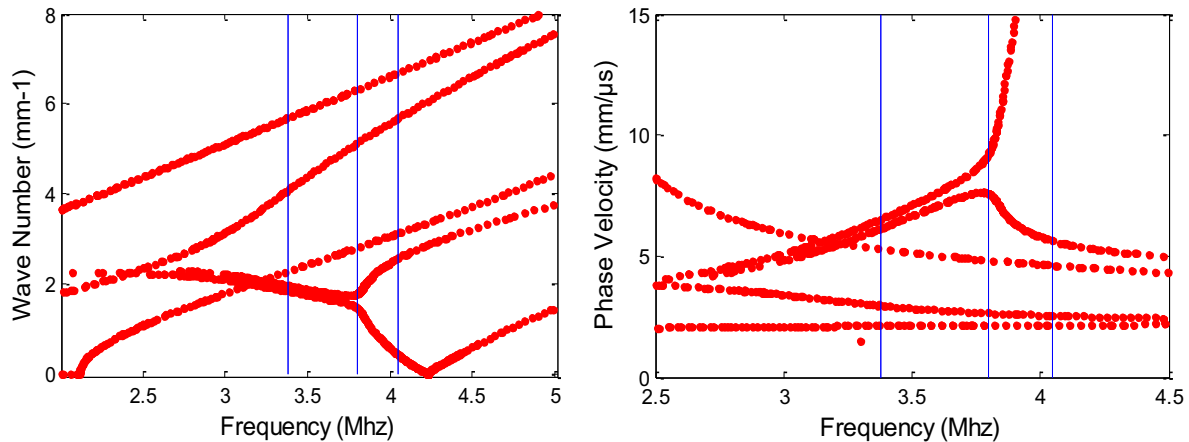


**FIGURE 4.** Dispersion curves of a half immersed plate of velocities  $V_L = 4.74 \text{ mm}/\mu\text{s}$  and  $V_T = 2.405 \text{ mm}/\mu\text{s}$  and thickness  $d = 0.57 \text{ mm}$ . The wavenumbers are displayed on the left and the phase velocities on the right. Blue lines indicate particular resonance frequencies observed in the experiment.

Figure 5 displays the echo after the transmission of a plane wave (first vector of the Hadamard basis). After a strong specular echo that has been saturated, the contributions of the guided modes are clearly visible and some of the modes circumnavigate several turns around the shell. It also appears that the signal does not vanish just after the specular echo meaning that some modes radiate immediately back to the array.

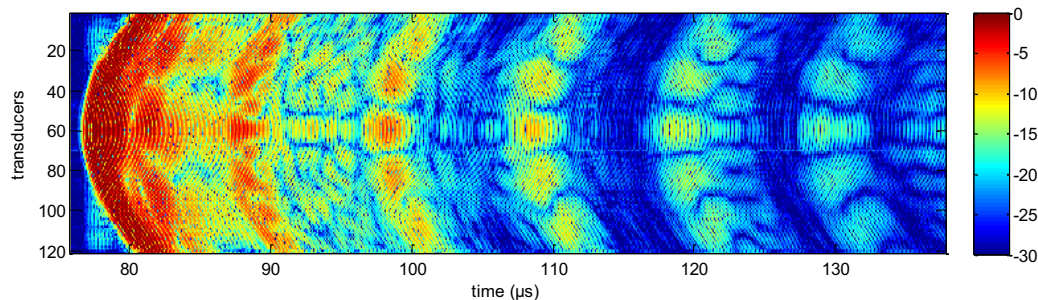


**FIGURE 5.** Echo of the zircaloy tube after transmission of a plane wave by all array elements. The specular echo has been saturated (the 4 first  $\mu\text{s}$ ). The radiations of the circumferential modes after several turns around the shell are clearly seen.

On each Bscan, a time window is applied to remove the specular echo. Then, after Fourier transform, the singular value decomposition of the array response matrix is calculated from 2.5 to 4.5 MHz. The singular values are plotted on Fig.6. Several resonances appear in this distribution. Below 3.7 MHz the set of regularly spaced resonances is similar to the one observed in reference 7. It corresponds to the  $A_1$  mode which circumnavigates several turns around the shell before vanishing. Below the resonance peaks, at least two other pairs of singular values are above noise. They correspond to  $A_0$  and  $S_0$  modes. This is confirmed by the back-propagation of the six first singular vectors as shown in figure 7. For example, the back-propagation of the first and second eigenvectors for the resonance at 3.38 MHz is focussed at two points that are separated by 2.5 mm. This corresponds to a value  $C_\phi = 5.6 \text{ mm}/\mu\text{s}$  which is the velocity of the  $A_1$  mode. For eigenvectors 3 and 4 the distance between focal points is 6.3 mm which corresponds to  $C_\phi = 2.22 \text{ mm}/\mu\text{s}$  and the  $A_0$  mode. For eigenvectors 5 and 6, the distance is 4.56 mm and corresponds to the  $S_0$  mode with  $C_\phi = 3.08 \text{ mm}/\mu\text{s}$ .

Two resonances appear at 3.79 and 4.05 MHz. Two singular values of the same amplitude form the first peak while the second one contains only one singular value. The first one is very close to the  $S_1S_2$ -ZGV resonance frequency measured in air by laser ultrasonics<sup>7</sup> and is associated with the quasi ZGV mode resonance. The back-propagations of the eigenvectors confirm this assertion. At 3.79 MHz, the first and second eigenvectors focuses on two points separated by 1.48 mm (Figure 8 left). This distance corresponds to a velocity of  $9.5 \text{ mm}/\mu\text{s}$  which is the phase velocity of the  $S_{25}$  mode.

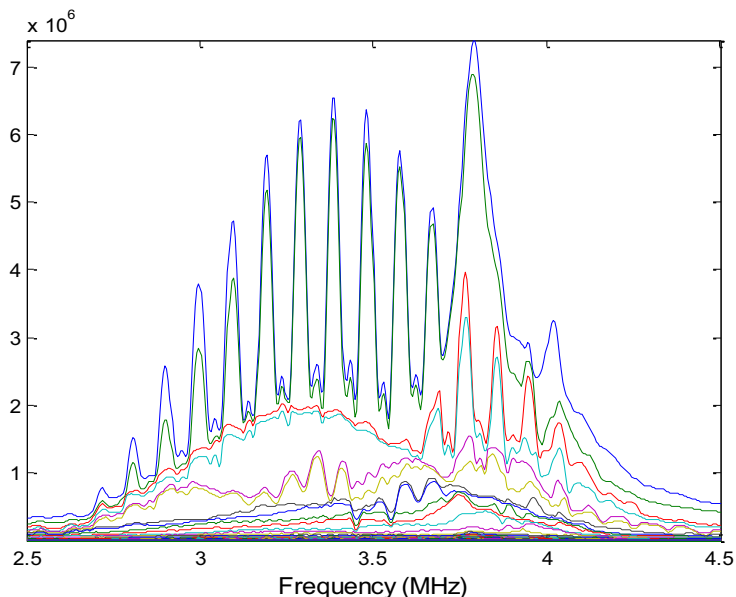


**FIGURE 6.** Backscattering by an air filled zircaloy hollow cylinder embedded in water : singular value of the array response matrix calculated after removing the specular echo.

At 4.05 MHz, the back-propagation of the first singular vector produces a single focal point, which corresponds an infinite (or at least very large) phase velocity (Figure 8 right). It is attributed to the longitudinal thickness resonance. For some unclear reason, this frequency is slightly smaller than the theoretical thickness resonance frequency  $V_L/2d=4.15\text{MHz}$ .

The backpropagation have also been calculated for all frequencies at the distance 62.5 mm. Figure 9 displays the sum of the back-propagation of the six first eigenvectors weighted by their corresponding singulars values, as a function of frequency. The different modes  $A_0$ ,  $A_1$  and  $S_1$  can easily be distinguished below 3.8 MHz. The two radiations points corresponding to the ZGV resonance dominate around 3.8MHz and the single point associated with the thickness resonance is clearly seen at 4.05 MHz.

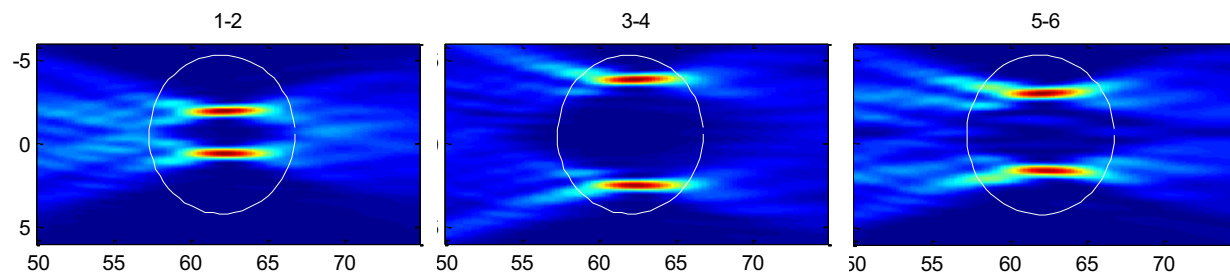


**FIGURE 7.** Back-propagation of the 6 first singular vectors at frequency 3.38 MHz. Three pairs of modes are observed :  $A_1$  associated with eigenvectors 1 and 2,  $A_0$  associated with eigenvectors 3 and 4, and  $S_0$  associated with eigenvectors 5 and 6. (axis are in mm).

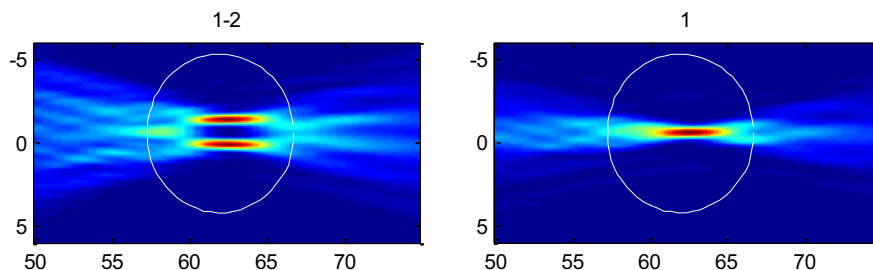


**FIGURE 8.** Back-propagation of the singular vectors 1 and 2 at frequency 3.79 MHz (left) and back-propagation of the first singular vector at frequency 4.05 MHz (right). Axis are in mm.

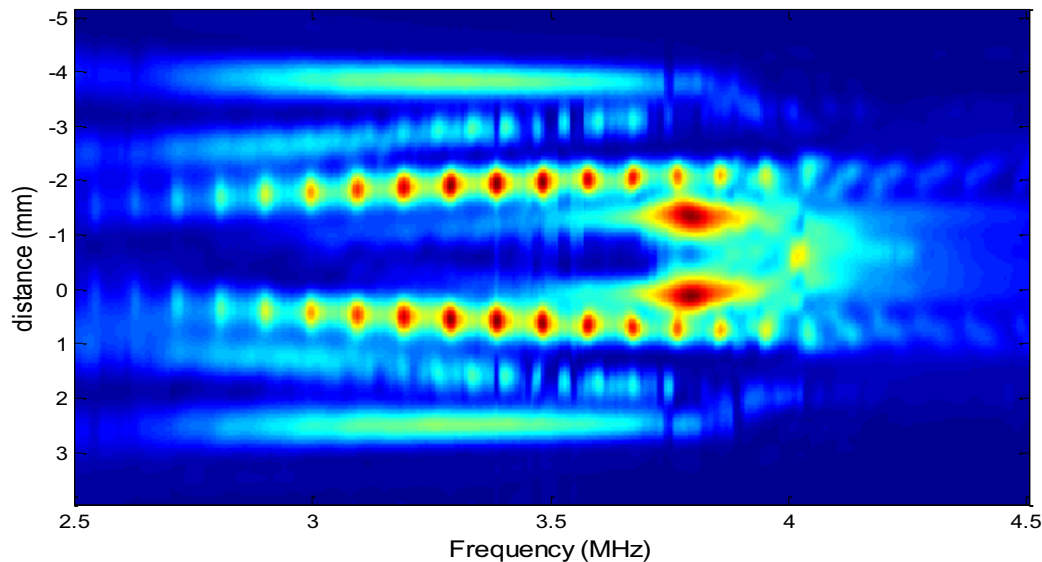


FIGURE 9. Sum of the back-propagations of the singular vectors 1 to 6 at the distance 62.5 mm from the array.

## CONCLUSION

A spatio-temporal analysis of the back-scattering by a hollow cylinder have been proposed. This analysis consists in studying the invariants of the time reversal operator measured by a linear array. Experimental results obtained on a zircaloy tube were presented. The different guided modes contributing to the back-scattering field were separated. The approach allowed the identification of the large contributions of the ZGV resonance and of the thickness resonance to the enhanced back-scattering.

Although, it was shown that the curvature does not change the  $S_{2b}$  mode for the zircaloy tube in air, it may be different when the tube is embedded in water. Consequently, the effect of curvature should be studied in further investigations.

## REFERENCES

1. G.S. Sammelman R. Hackmann "The acoustic scattering by a submerged, spherical shell. II: The high-frequency region and the thickness quasi-resonance", *J. Acoust. Soc. Am.* **89** (5), (1991)
2. G. Kaduchak, DH. Hughes, PL. Marston, "Enhancement of the backscattering of high-frequency tone bursts by thin spherical shells associated with a backwards wave – observations and ray approximation", *J. Acoust. Soc. Am.* **96** (6) 3704-3741 (1994).
3. G. Kaduchak, PL. Marston, "Traveling-wave decomposition of surface displacements associated with scattering by a cylindrical shell: Numerical evaluation displaying guided forward and backward wave properties" *J. Acoust. Soc. Am.* **98** (6) 3501-3507 (1995).
4. A.H. Meitzler, "Backward wave transmission of stress pulses in elastic cylinder and plates", *J. Acoust. Soc. Am.* **38** (5) (1965).
5. M. Germano, A. Alippi, M. Angelici, and A. Bettucci, "Self-interference between forward and backward propagating parts of a single acoustic plate mode", *Phys. Rev. E*, (**65**), 046608, (2002)
6. P.L. Marston "Negative group velocity Lamb waves on plates and applications to the scattering of sound by shells" *J. Acoust. Soc. Am.* **113** (5) 2659-2662 (2003)
7. C. Prada, and M. Fink, "Separation of interfering acoustic scattered signals using the invariants of the time-reversal operator. Application to Lamb waves characterization." *J. Acoust. Soc. Am.* **104** 801-807 (1998)
8. M. Cès, D. Royer, C. Prada, "Characterization of mechanical properties of a hollow cylinder with zero group velocity Lamb modes", *J. Acoust. Soc. Am.* **132** (1), (2012)